Large Third-Order Optical Nonlinearity of Cu-O Chains Investigated by Third-Harmonic Generation Spectroscopy

H. Kishida,[1] M. Ono,[1] K. Miura,[1] H. Okamoto,[1,2,3] M. Izumi,[4] T. Manako,[4] M. Kawasaki,[2,4,5] Y. Taguchi,[6] Y. Tokura,[2,4,6] T. Tohyama,[5] K. Tsutsui,[5] and S. Maekawa[5]

[1]*Department of Advanced Materials Science, University of Tokyo, Tokyo 113-0033, Japan*

[2]*Correlated Electron Research Center (CERC), National Institute of Advanced Industrial Science and Technology (AIST), Tsukuba, 305-0046 Japan*

[3]*Structure and Transformation Group, PRESTO, Tokyo 113-0033, Japan*

[4]*Joint Research Center for Atom Technology (JRCAT), Tsukuba 305-0046, Japan*

[5]*Institute for Materials Research, Tohoku University, Sendai 980-8577, Japan*

[6]*Department of Applied Physics, University of Tokyo, Tokyo 113-8656, Japan*

(Received 16 January 2001; published 8 October 2001)

Spectra of the third-order nonlinear susceptibility $\chi^{(3)}$ have been investigated for one-dimensional Mott insulators, Sr_2CuO_3 and Ca_2CuO_3, by applying the third-harmonic generation (THG) spectroscopy on their single-crystalline thin films. The three-photon resonance to the lowest charge-transfer (CT) state with odd parity strongly enhances $\chi^{(3)}$, which is of the order of 10^{-9} esu. The two-photon resonant structure unravels the even-CT state, located close to the odd-CT state. Two types of $\chi^{(3)}$ spectra obtained from THG and the electroreflectance measurements are explained based on the concept of spin-charge separation.

DOI: 10.1103/PhysRevLett.87.177401 PACS numbers: 78.66.Nk, 42.65.Ky

Semiconductors with one-dimensional (1D) electronic structure have been of particular importance in nonlinear optics, since the motion of electrons in a confined space can give rise to large optical nonlinearity [1,2]. Numerous studies about the third-order nonlinear optical susceptibility $\chi^{(3)}$ have been devoted to conjugated polymers [3–7]. Recently, it has been reported that $\chi^{(3)}$ is anomalously enhanced in another type of 1D material, that is, 1D Mott insulators of copper oxide, Sr_2CuO_3 [8,9], and halogen-bridged Ni^{3+}-chain compounds [8]. In these materials, the Mott-Hubbard gap is opened in the d band of copper (or nickel) due to the large on-site Coulomb interaction U on the metal sites. Charge transfer (CT) transitions from oxygen (or halogen) to copper (or nickel) correspond to the optical gap of 1–2 eV in these compounds. In the study [8], $\chi^{(3)}(-\omega;0,0,\omega)$ reach 10^{-8} to 10^{-5} esu, which is defined via the relation, $P(\omega) = 3\epsilon_0\chi^{(3)}(-\omega;0,0,\omega)E(0)^2E(\omega)$, and deduced from the electroreflectance (ER) measurements. Here, $P(\omega)$ shows nonlinear polarization, $E(0)$ shows the static electric field, $E(\omega)$ shows the electric field of light, and ϵ_0 shows the permittivity of vacuum. The analysis of $\chi^{(3)}(-\omega;0,0,\omega)$ spectra based on a three-level model has suggested that odd- and even-CT states are nearly degenerate and that the enhancement of $\chi^{(3)}$ is due to a large transition dipole moment between these two CT states. In fact, the even-CT state has been unambigously demonstrated in Sr_2CuO_3 [9] by measurements of the two-photon absorption resonance corresponding to $\mathrm{Im}\chi^{(3)}(-\omega_1;-\omega_2,\omega_2,\omega_1)$.

The most useful method for the quantitative evaluation of $\chi^{(3)}$ by purely optical processes (without static electric field) is third-harmonic generation (THG) spectroscopy. In this method, both one-photon allowed states with odd parity and one-photon forbidden states with even parity can be detected via multiphoton resonant processes.

In this Letter, we report $|\chi^{(3)}(-3\omega;\omega,\omega,\omega)|$ spectra of the oriented thin films of Sr_2CuO_3 and Ca_2CuO_3 investigated by the THG spectroscopy. $|\chi^{(3)}(-3\omega;\omega,\omega,\omega)|$ is defined by $P(3\omega) = \frac{1}{4}\epsilon_0\chi^{(3)}(-3\omega;\omega,\omega,\omega)E(\omega)^3$. The $|\chi^{(3)}(-3\omega;\omega,\omega,\omega)|$ spectra show clearly the structures due to the three-photon resonance to odd-CT state and the two-photon resonance to even-CT state. Spectral shapes of $|\chi^{(3)}(-3\omega;\omega,\omega,\omega)|$ and $\mathrm{Im}\chi^{(3)}(-\omega;0,0,\omega)$ are explained by using the concept of holon and doublon, which are positively and negatively charged spinless carriers created as optical excited species in spin-charge separation. By comparing the nonlinear optical spectra of the two 1D cuprates with the calculated spectra based on the holon-doublon model, we show a crossover behavior from the excitonic bound states of holon and doublon to the unbound continuum excited states with an increase of the nearest-neighbor hopping t along the Cu-O chain.

Sr_2CuO_3 and Ca_2CuO_3 share the common crystal structure shown in Fig. 1(a). 1D Cu-O chains are composed of CuO_4 quadrilateral structures sharing corner oxygens along the b axis. The lattice constants of Ca_2CuO_3 are smaller than those of Sr_2CuO_3 as listed in Fig. 1(c). The thin films for THG measurements were fabricated by a graphoepitaxial laser ablation technique [10]. In this method, we obtained the oriented films on the anisotropic substrate, $LaSrAlO_4$, by using the lattice matching between the 1D cuprates and the substrates. The thickness of the film is 800 Å for Sr_2CuO_3 and 385 Å for Ca_2CuO_3. For protection, we coated the cuprate layer with 1000 Å of $LaAlO_3$. Bulk single crystals of Sr_2CuO_3 and Ca_2CuO_3

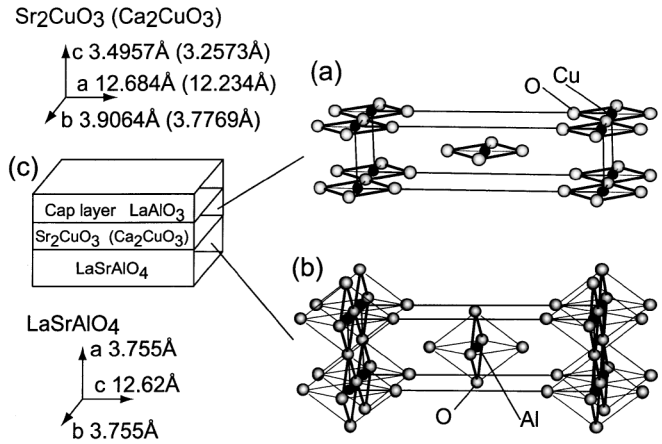

FIG. 1. Crystal structure of Sr_2CuO_3 (Ca_2CuO_3) (a) and $LaSrAlO_4$ (b). For simplicity, Sr(Ca) and La atoms are omitted. The layer structure of the sample is illustrated in (c).

for ER measurements were grown by the traveling-solvent floating-zone method and the flux method, respectively.

In the THG measurements, we used light pulses with 6 nsec duration obtained from the combination of a Q-switched Nd:YAG laser and a tunable optical parametric oscillator system. To evaluate the absolute value of $|\chi^{(3)}(-3\omega;\omega,\omega,\omega)|$, we compared the TH intensity from the thin films with that from SiO_2, both of which were measured by the Maker-fringe method [11]. The $\chi^{(3)}$ spectrum of SiO_2 is calculated by applying Miller's rule [12,13] to the reported value at 1.907 μm [14]. $\mathrm{Im}\chi^{(3)}(-\omega;0,0,\omega)$ are obtained from the ER measurements. The detail of the ER experiment was described elsewhere [8].

In Figs. 2(a) and 2(b), we show the polarized absorption spectra of the thin films. In the spectra with the electric field of light $E \parallel$ chain, the peak structures are observed at about 1.75 eV in Sr_2CuO_3 and 2.10 eV in Ca_2CuO_3. They are assigned to the CT gap transition from the filled oxygen $2p$ band to the copper 3 d upper Hubbard band. On the other hand, there are no distinct structures in the absorption spectra with $E \perp$ chain. Such a strong anisotropy ensures the 1D alignment of Cu-O chains.

$|\chi^{(3)}(-3\omega;\omega,\omega,\omega)|$ spectra of the thin films for $E \parallel$ chain are shown in Figs. 2(c) and 2(d). In Sr_2CuO_3, a sharp peak A at $\omega_A = 0.61$ eV and a hump structure B at $\omega_B = 0.87$ eV are observed. The $|\chi^{(3)}(-3\omega;\omega,\omega,\omega)|$ value at ω_A reaches 1×10^{-9} esu. This is comparable to the maximum value of $|\chi^{(3)}(-3\omega;\omega,\omega,\omega)|$ in polydiacetylene, which is one of the representatives of third-order nonlinear optical materials [15]. The two structures A and B in the $|\chi^{(3)}(-3\omega;\omega,\omega,\omega)|$ spectrum of Sr_2CuO_3 should be related to multiphoton resonant processes. In THG, there can be three types of resonances, that is, one-, two-, and three-photon resonances, to specific energy levels. We can exclude the contributions of the one-photon resonance process, since ω_A and ω_B are much lower than the absorption edge. ω_A is one-third

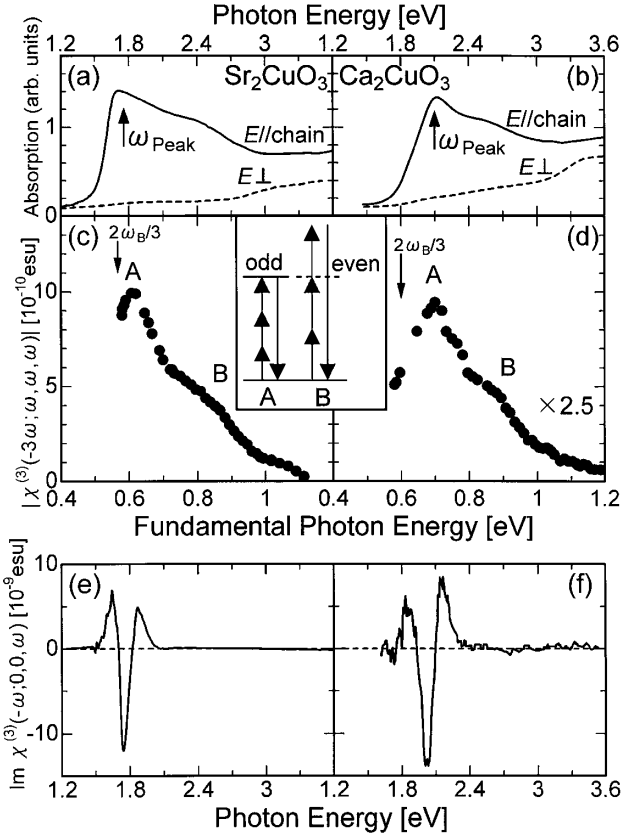

FIG. 2. Polarized absorption spectra (a),(b) with light polarization $(E) \parallel$ and $\perp$ chain and $|\chi^{(3)}(-3\omega;\omega,\omega,\omega)|$ spectra (c),(d) with $E \parallel$ chain in thin film samples of 1D cuprates. Inset: the three-photon resonance to the odd-CT state and the two-photon resonance to the even-CT state are illustrated. The $\mathrm{Im}\chi^{(3)}(-\omega;0,0,\omega)$ spectra measured at 77 K with E and applied electric field $(F) \parallel$ chain are shown in (e) and (f).

of the absorption peak energies, so that the peak A can be assigned to the three-photon resonant structure to the lowest CT state with odd parity. As for the structure B, it is necessary to take into account the possibility of two-photon resonance as well as three-photon resonance. To clarify which process is dominant, we will refer to the results of $\mathrm{Im}\chi^{(3)}(-\omega;0,0,\omega)$.

In Figs. 2(e) and 3(c), we show the $\mathrm{Im}\chi^{(3)}(-\omega;0,0,\omega)$ spectrum of Sr_2CuO_3. In the spectrum, there is an oscillating structure at about 1.7 eV ($\approx 2\omega_B$). It is to be noted, by contrast, that there is no structure at about 2.6 eV ($\approx 3\omega_B$). Thus, there exists no excited state contributing to the nonlinear optical process in the energy region at about $3\omega_B$. These results strongly suggest that the structure B observed in the $|\chi^{(3)}(-3\omega;\omega,\omega,\omega)|$ spectrum should be attributed not to the three-photon resonance to some odd-parity states ($3\omega_B$), but to the two-photon resonance to the even-parity state ($2\omega_B$) hidden near the one-photon allowed CT peak ($3\omega_A \sim \omega_{\mathrm{peak}}$). The two- and three-photon resonance processes in THG are illustrated in the inset of Fig. 2.

In Ca_2CuO_3, spectral shapes of $|\chi^{(3)}(-3\omega;\omega,\omega,\omega)|$ [Fig. 2(d)] and $\mathrm{Im}\chi^{(3)}(-\omega;0,0,\omega)$ [Figs. 2(f) and 3(d)]

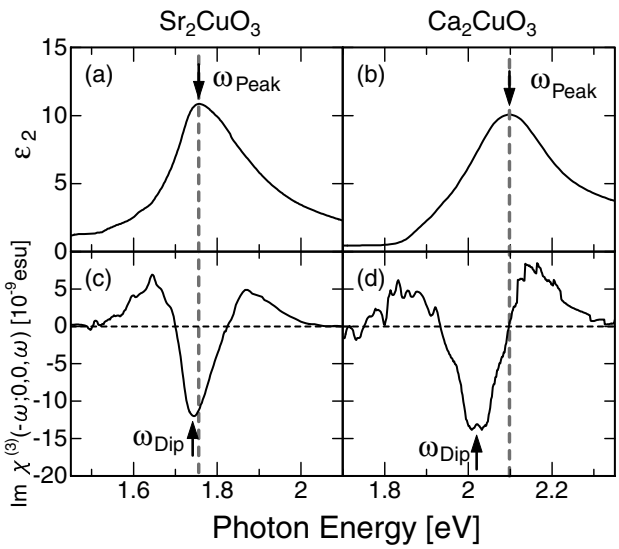

FIG. 3. ϵ_2 (upper panels) and $\mathrm{Im}\chi^{(3)}(-\omega;0,0,\omega)$ (lower panels) spectra at 77 K in the single-crystal samples of Sr_2CuO_3 (a),(c) and Ca_2CuO_3 (b),(d).

are similar to those observed in Sr_2CuO_3. In analogy to the case of Sr_2CuO_3, the structure A at $\omega_A = 0.70$ eV and the B at $\omega_B = 0.90$ eV are attributable to the three-photon resonance to the odd-CT state and the two-photon resonance to the even-CT state, respectively. Comparing the energy positions in more detail, however, some differences can be discerned between the two 1D cuprates. First, the energy of the minimum ω_{dip} in $\mathrm{Im}\chi^{(3)}(-\omega;0,0,\omega)$, which characterizes the energy position of the oscillating structure, is almost equal to ω_{peak} in Sr_2CuO_3, but slightly smaller than ω_{peak} in Ca_2CuO_3. Second, $2\omega_B$ is almost equal to $3\omega_A$ in Sr_2CuO_3, but smaller than $3\omega_A$ in Ca_2CuO_3. The energy positions of $2\omega_B/3$ are indicated by the arrows in Figs. 2(c) and 2(d). These differences are attributable to the difference in the Cu-O bond length along the 1D chains.

It is well established that the CT transitions in insulating cuprates can be described by a half-filled Hubbard model with a single band by mapping a bound state with mainly oxygen $2p$ character (the Zhang-Rice state) onto the lower Hubbard band [16]. Therefore, to unravel the physics behind the different behaviors in $\chi^{(3)}$ between the two compounds, we use the half-filled 1D Hubbard chain with large on-site Coulomb interaction U, nearest-neighbor Coulomb interaction V, and nearest-neighbor hopping matrix element t, which can capture the essence of the low-lying optical excitations in the cuprates. In the strong coupling limit $U/t \gg 1$, two types of carriers are created in the excitation process across the Mott gap: one is an unoccupied site with positive charge and the other is a doubly occupied site with negative charge. Because of the nature of the spin-charge separation inherent in 1D systems [16], they have only charge degrees of freedom and are called holon and doublon, respectively. These two carriers attract each other by $-V$, and thus we have an effective two-particle model with the charge degrees of freedom and no spin degree [17]. We call it the holon-doublon model [18]. The two particles in the model cannot occupy the same site because of the large on-site Coulomb interaction. This is in contrast with a standard exciton model of 1D semiconductors which allows the occupation of a particle and a hole at the same site. The prohibition of the double occupancy necessarily induces a node of the envelope wave function at the origin of relative coordinates, and the odd- and even-parity states are always degenerate under the presence of the node [18]. In the calculation of the nonlinear susceptibilities, the initial state before photoexcitation is regarded as a vacuum state without holon and doublon. The dipole moment between the vacuum state and the odd-parity eigenstate of the holon-doublon model is calculated through the current process creating a holon and doublon pair on the adjacent sites. All of the eigenstates of the model are obtained by numerically diagonalizing the Hamiltonian for a given chain. The calculation based on this model makes possible the direct comparison of the spectral shape between the experimental and calculated results.

The values of the parameters in the holon-doublon model have been evaluated for Sr_2CuO_3 from the analysis of electron energy loss spectroscopy spectra ($t = 0.55$, $V = 1.3$, and $U = 4.2$ in units of eV) [19]. As denoted in Fig. 1, the Cu-O bond length along the chain is smaller in Ca_2CuO_3 than in Sr_2CuO_3. This implies that both V and t are larger in Ca_2CuO_3. However, t is expected to be more sensitive to the bond length than V [20]. Therefore, to investigate the material dependence of the nonlinear susceptibilities, the value of V in this paper is fixed to be 1, and t is changed from $1/3$ to 1 in the following calculations. The value of U is determined so as to satisfy $U - 4t = 2$.

Figure 4 shows calculated ϵ_2, $\mathrm{Im}\chi^{(3)}(-\omega;0,0,\omega)$, and $|\chi^{(3)}(-3\omega;\omega,\omega,\omega)|$ for a 100-site chain with the damping factor of 0.15. In ϵ_2, the energy distribution of the square of the dipole moments from the ground states is also shown by vertical bars. It is known that, when $V/t > 2$, an excitonic bound state splits off from the lower edge of a continuum spectrum at $\omega = U - 4t$ [17]. In fact, a bound state is formed at $\omega = 1.9$ for $t = 1/3$ ($V/t = 3$) in ϵ_2. With increasing t, the energy of the peak in ϵ_2, ω_{peak}, indicated by dashed lines shifts to higher energy beyond the lower edge of the continuum at $\omega = 2$, indicated by the triangles. For $t = 1/3$, the energy of the dip, ω_{dip}, in $\mathrm{Im}\chi^{(3)}(-\omega;0,0,\omega)$ is almost equal to ω_{peak} in ϵ_2. With increasing t, ω_{dip} shifts to higher energy. However, in contrast to ω_{peak}, ω_{dip} is pinned near the edge at $\omega = 2$. This is due to the presence of even-parity states degenerate with odd-parity states near the edge. Therefore, the energy difference between ω_{dip} and ω_{peak} increases with the increase of t. This tendency explains the experimental fact that ω_{dip} is almost equal to ω_{peak} in Sr_2CuO_3 but smaller than ω_{peak} in Ca_2CuO_3.

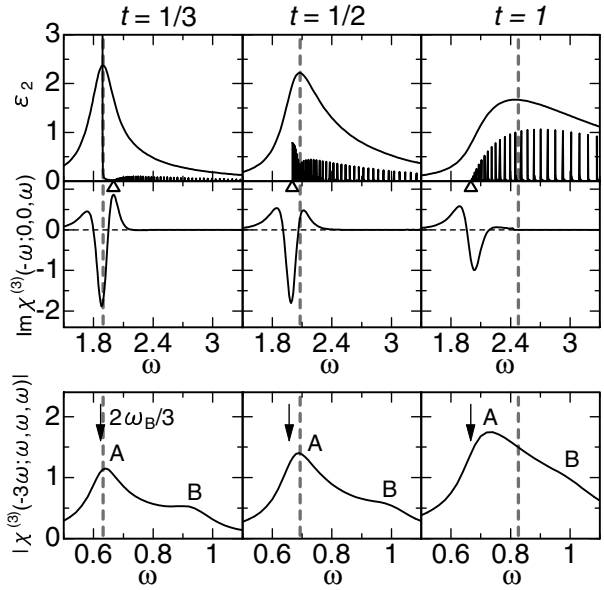

FIG. 4. ϵ_2, $\mathrm{Im}\chi^{(3)}(-\omega;0,0,\omega)$, and $|\chi^{(3)}(-3\omega;\omega,\omega,\omega)|$ in the holon-doublon model for a 100-site chain with $t = 1/3$, $1/2$, and 1. $V = 1$ for all the parameter sets. The value of U is determined so as to satisfy $U - 4t = 2$, which gives the lower edge of the continuum spectra denoted by the triangles. The damping factor is set to be 0.15. In ϵ_2, the energy distribution of the square of the dipole moments from the ground states is also shown by vertical bars. In $|\chi^{(3)}(-3\omega;\omega,\omega,\omega)|$, the positions of $2\omega_B/3$ are shown by the arrows, where ω_B is the energy of the hump structure B.

In the calculated spectra of $|\chi^{(3)}(-3\omega;\omega,\omega,\omega)|$, a sharp peak due to three-photon resonance and a broad hump structure due to two-photon resonance are clearly observed, which are in accordance with the experiments. ω_A for $t = 1/3$ is nearly equal to $\omega_{\mathrm{peak}}/3$, while ω_A becomes lower than $\omega_{\mathrm{peak}}/3$ with increasing t. This means that the peak position of the three-photon resonance structure does not necessarily coincide with the peak position of ϵ_2. Moreover, for comparison with ω_{A}, the positions of $2\omega_B/3$ are denoted by arrows. With increasing t, the difference $3\omega_A - 2\omega_B$ increases. This behavior is again consistent with the experimental result that $2\omega_B$ is slightly smaller than $3\omega_A$ in Ca_2CuO_3, while $2\omega_B \sim 3\omega_A$ in Sr_2CuO_3. This fact strongly suggests that the character of the excited state changes from the excitonic bound states of holon and doublon in Sr_2CuO_3 to the unbound continuum excited states in Ca_2CuO_3.

In summary, we have presented the third-order nonlinear susceptibility $|\chi^{(3)}(-3\omega;\omega,\omega,\omega)|$ spectra of Sr_2CuO_3 and Ca_2CuO_3 obtained from the THG spectroscopy. The observed two distinct structures have been attributed to the three-photon resonance to the odd-CT state and the two-photon resonance to the even-CT state. By using the holon-doublon model, two types of $\chi^{(3)}$ spectra obtained from THG and ER spectroscopy have been well reproduced, in spite of the fact that they correspond to the optical responses in completely different frequency regions. This ensures the validity of the present analysis. Moreover, the difference of the spectral shape of $\chi^{(3)}$ between Sr_2CuO_3 and Ca_2CuO_3 has been explained by taking account of the change in the nearest-neighbor hopping t. A crossover behavior from the excitonic bound states of holon and doublon to the unbound continuum excited states is the physics behind the difference between the two compounds.

This work was supported by a Grant-In-Aid from the Ministry of Education, Science, Sports and Culture of Japan, CREST, and NEDO. The numerical calculations were performed in the supercomputing facilities of ISSP, University of Tokyo, and IMR, Tohoku University.

[1] D. H. Auston *et al.,* Appl. Opt. **26**, 211 (1987).
[2] C. Sauteret *et al.,* Phys. Rev. Lett. **36**, 956 (1976).
[3] W.-S. Fann *et al.,* Phys. Rev. Lett. **62**, 1492 (1989).
[4] T. Hasegawa *et al.,* Phys. Rev. Lett. **69**, 668 (1992).
[5] C. Halvorson *et al.,* Chem. Phys. Lett. **200**, 364 (1992).
[6] S. V. Frolov *et al.,* Phys. Rev. Lett. **85**, 2196 (2000).
[7] S. N. Dixit, D. Guo, and S. Mazumdar, Phys. Rev. B **43**, 6781 (1991).
[8] H. Kishida *et al.,* Nature (London) **405**, 929 (2000).
[9] T. Ogasawara *et al.,* Phys. Rev. Lett. **85**, 2204 (2000).
[10] S. Miyazawa and M. Mukaida, Appl. Phys. Lett. **64**, 2160 (1994).
[11] F. Kajzar, J. Messier, and C. Rosilio, J. Appl. Phys. **60**, 3040 (1986).
[12] R. C. Miller, Appl. Phys. Lett. **5**, 17 (1964).
[13] C. G. B. Garrett and F. N. H. Robinson, IEEE J. Quantum Electron. **QE-2**, 328 (1966).
[14] B. Buchalter and G. R. Meredith, Appl. Opt. **21**, 3221 (1982).
[15] T. Kanetake *et al.,* Appl. Phys. Lett. **54**, 2287 (1989).
[16] S. Maekawa and T. Tohyama, Rep. Prog. Phys. **64**, 383 (2001), and references therein.
[17] W. Stephan and K. Penc, Phys. Rev. B **54**, R17 269 (1996); F. Gebhard *et al.,* Philos. Mag. B **75**, 47 (1997).
[18] Y. Mizuno *et al.,* Phys. Rev. B **62**, R4769 (2000).
[19] R. Neudert *et al.,* Phys. Rev. Lett. **81**, 657 (1998).
[20] W. A. Harrison, *Electronic Structure and the Properties of Solids: The Physics of the Chemical Bond* (Freeman, San Francisco, 1980).